



# Kent Academic Repository

**Bai, Lu, Pepper, Matthew G., Yan, Yong, Spurgeon, Sarah K., Sakel, Mohamed and Phillips, Malcolm (2015) *Quantitative Assessment of Upper Limb Motion in Neurorehabilitation Utilizing Inertial Sensors*. IEEE Transactions on Neural Systems and Rehabilitation Engineering . pp. 232-243. ISSN 1534-4320.**

## Downloaded from

<https://kar.kent.ac.uk/47726/> The University of Kent's Academic Repository KAR

## The version of record is available from

<https://doi.org/10.1109/TNSRE.2014.2369740>

## This document version

UNSPECIFIED

## DOI for this version

## Licence for this version

UNSPECIFIED

## Additional information

## Versions of research works

### Versions of Record

If this version is the version of record, it is the same as the published version available on the publisher's web site. Cite as the published version.

### Author Accepted Manuscripts

If this document is identified as the Author Accepted Manuscript it is the version after peer review but before type setting, copy editing or publisher branding. Cite as Surname, Initial. (Year) 'Title of article'. To be published in *Title of Journal*, Volume and issue numbers [peer-reviewed accepted version]. Available at: DOI or URL (Accessed: date).

## Enquiries

If you have questions about this document contact [ResearchSupport@kent.ac.uk](mailto:ResearchSupport@kent.ac.uk). Please include the URL of the record in KAR. If you believe that your, or a third party's rights have been compromised through this document please see our [Take Down policy](https://www.kent.ac.uk/guides/kar-the-kent-academic-repository#policies) (available from <https://www.kent.ac.uk/guides/kar-the-kent-academic-repository#policies>).

# Quantitative Assessment of Upper Limb Motion in Neurorehabilitation Utilizing Inertial Sensors

Lu Bai, Matthew G. Pepper, Yong Yan, *Fellow, IEEE*, Sarah K. Spurgeon, *Senior Member, IEEE*, Mohamed Sakel and Malcolm Phillips

**Abstract**— Two inertial sensor systems were developed for 3D tracking of upper limb movement. One utilizes four sensors and a Kinematic model to track the positions of all four upper limb segments/joints and the other uses one sensor and a Dead Reckoning algorithm to track a single upper limb segment/joint. Initial evaluation indicates that the system using the Kinematic Model is able to track orientation to 1 degree and position to within 0.1 cm over a distance of 10 cm. The dead reckoning system combined with the ‘Zero Velocity Update’ correction can reduce errors introduced through double integration of errors in the estimate in offsets of the acceleration from several meters to 0.8% of the total movement distance. Preliminary evaluation of the systems has been carried out on ten healthy volunteers and the Kinematic System has also been evaluated on one patient undergoing neurorehabilitation over a period of ten weeks. The initial evaluation of the two systems also shows that they can monitor dynamic information of joint rotation and position and assess rehabilitation process in an objective way, providing additional clinical insight into the rehabilitation process.

**Index Terms**—3D motion tracking, dead reckoning, inertial sensors, kinematic modelling, motion monitoring, upper limb motion, Zero Velocity Update.

## I. INTRODUCTION

ABOUT 10 million people in the UK live with a neurological condition e.g. stroke, traumatic brain injury, and motor neurone disease [1]. Neurological conditions and disorders can result in mental and physical disabilities and one outcome can be dysfunction of upper limb function [2]. The recovery of upper limb function is of great importance in improving the patients’ quality of life and helping them to maximize their independence [3]. Rehabilitation, which usually includes occupational therapy and physiotherapy, can help to ease symptoms, and restore upper limb function. Assessment of recovery

is an important aspect of any rehabilitation program. In general, most of the currently available assessments are viewed and scored by therapists based on assessment scales and decision rules. For example, the Fugl-Meyer Assessment (FMA) [4], the Box & Block Test (BBT) [5] and the Action Research Arm Test (ARAT) [6] are all thought to be comprehensive and quantitative measures of upper limb motor function, having been used for years. Although these assessments have proven to be effective and reliable [7] [8], they do not provide objective data on the physical movement of the upper limb or how the upper limb moves through space. Therefore, there is considerable interest in developing motion tracking systems as a tool for the quantitative measurement of dynamic upper limb movement [9] [10]. This precise data may add value in monitoring progress of the patient and the rehabilitation program.

Developing a motion monitoring system for clinical use a hospital setting must be acceptable to patient and clinician. Ideally the system should be transportable, easy to set up, and have minimal impact on the patients’ normal range of movement. Existing motion tracking systems can be divided into two types: visual tracking and non-visual tracking systems. Visual or video tracking systems are well proven for motion analysis and meet the requirements for upper limb tracking [11]. However, they are relatively complex, expensive and require careful setup. There are also several non-visual tracking technologies available that are based on inertial, mechanical, acoustic and magnetic sensing strategies [12] [13]. Mechanical sensing systems could provide a straightforward way to track the joints but they are uncomfortable to wear for long periods. Acoustic sensing and magnetic sensing are affected by ambient conditions e.g. temperature, humidity or surrounding conductive/magnetic materials [14]. However, recent advances in inertial sensing technology based on micro-machined electromechanical systems (MEMS) [15] have made the use of small and lightweight inertial sensors a viable option.

A number of studies have used inertial sensors and kinematic modelling for human upper limb motion tracking - including Zhou, et al. [16], Hingtgen, et al. [17] and Perry, et al. [18]. At least two sensors (on upper arm and forearm segments to monitor the elbow and wrist orientation) are required to construct a basic upper limb link kinematic model. In Zhou, et al. [16], a two-sensor system is used and the shoulder movement is predicted by an optimization technique without requiring an additional sensor on the shoulder. But other motion data

Manuscript received October 15, 2013; revised May 13, 2014 and July 21, 2014; accepted September 04, 2014. This work was supported by the East Kent Hospitals University NHS Foundation Trust Internal Research Grant Scheme.

L. Bai, Y. Yan, and S. K. Spurgeon are with the School of Engineering and Digital Arts, University of Kent, CT2 7NT Canterbury, U.K. (e-mail: L.Bai@kent.ac.uk; Y.Yan@kent.ac.uk; S.K.Spurgeon@kent.ac.uk).

M. G. Pepper is with the School of Engineering and Digital Arts, University of Kent, CT2 7NT Canterbury, U.K. He is also with East Kent Hospitals University NHS Foundation Trust, CT1 3NG Canterbury, U.K. (e-mail: M.G.Pepper@kent.ac.uk; matthew.pepper@nhs.net).

M. Sakel and M. Phillips are with East Kent Hospitals University NHS Foundation Trust, CT1 3NG Canterbury, U.K. (e-mail: msakel@nhs.net; malcolm.phillips@nhs.net).

(e.g. angular velocity, orientation and acceleration) from the shoulder cannot be obtained. Therefore, in order to measure and then analyze the motion of all the upper limb segments (hand, wrist, elbow and shoulder), a kinematic model using at least four inertial sensors is required. Although the four - inertial sensor system enables the accurate tracking for all the upper limb segments, it has the disadvantages of its high cost (£6000) and the complexity of the system set-up. Under some circumstances it may only be necessary to monitor the motion of a single segment. Theoretically this could be achieved using one sensor and the Dead Reckoning (DR) method [19] based on strapdown inertial navigation technology [20]. This has been used in pedestrian tracking in indoor navigation [21] [22]. Additionally reducing the number of the sensors to one would benefit both patients and clinicians in terms of complexity, cost and burden on the patient. However, one of the major challenges in using Dead Reckoning is the need to minimize the drift in estimate of position resulting from the double integration of errors in the estimate of offsets in the linear acceleration. There are a range of options available, one of which is the Zero Velocity Update (ZUPT) [23], this technique has been used in pedestrian position tracking and is based on the identification of zero velocity intervals of the foot during the stance and swing phases of walking [22]. Unlike walking, clear zero velocity intervals may not always exist for upper limb movement assessments. However, for some of the assessment tests there are known events when the limb segments are stationary, e.g. during peg collection and placement in the nine-hole peg test (NHPT) [24]. Therefore the ZUPT technique has been applied in this preliminary evaluation of the inertial measurement system using a single sensor and the DR method. Additionally, these two systems are able to provide more information on the active range of motion (AROM) measurement. AROM is considered to be a good indicator of response to the rehabilitation program and for differentiating between individuals [25]. The standard measurement device, the goniometer [26], provides the clinician with a static measurement of the overall AROM, typically within  $1^\circ$ , but cannot provide any data on how that motion was achieved. However the use of the inertial motion measurement system also provides dynamic information throughout the movement, typically to within  $1^\circ$  [27].

As some of the researchers have introduced the quantitative tool into treatment regimes [28], in this research inertial tracking systems have been developed to enable clinicians to obtain repeatable and objective measurements of the progress and efficacy of rehabilitation interventions, including the use of botulinum therapy or functional electrical stimulation [29] [30]. As stated previously, the implementation of the four-sensor system is able to track all the upper limb segments. This will provide the clinician with complete motion information of the upper limb segments. The single sensor system reduces the complexity of measurement system, and enables the tracking of a specific joint and limb segment. Once the two systems have been evaluated the aim of this research is to investigate whether these system are able to obtain novel quantitative motion information from patients' assessment during

rehabilitation. It also should be noted that these sensors should be acceptable to patients, and measurement systems utilizing these sensors must also be suitable for use in the hospital environment, be portable and easy to set up.

## II. METHODS

### A. System Setup

The two motion tracking systems use the Xsens MTx [27] inertial sensor which was developed for use in biomechanics [31]. The MTx sensor contains two biaxial-accelerometers (ADXL202E), three single-axis gyroscopes (ENC-03J) and three magneto-resistive sensors (KMZ51). This combination enables the measurement of 3D acceleration, 3D magnetic field and 3D angular velocity. Furthermore, Xsens have embedded a calibration and a Kalman Filter (XKF) sensor fusion algorithm Xsens in the MTx which can be applied to the raw data to provide an accurate estimation of sensor 3D orientation.

The inertial sensing system set up is illustrated in Fig. 1. The four sensors are connected by cables to the Xbus master which provides the sensors with power and connection to a PC running the Xsens MT (Motion Tracking) manager software development kit [32]. The maximum sampling frequency for the raw data is 512 Hz per sensor. The maximum sampling frequency for the calibrated data is reduced to 120 Hz per sensor, and is sufficient to capture human upper limb movement. Matlab (2009b, The MathWorks) was used for data pro-

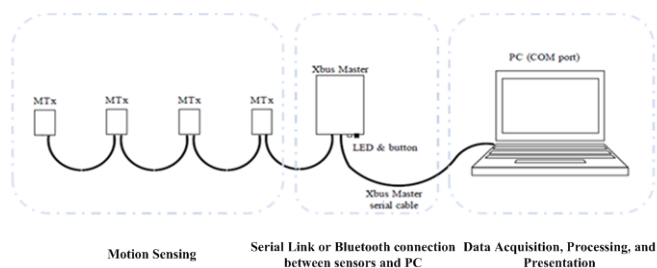


Fig. 1. Structure of the motion tracking system

cessing, analysis and presentation.

The parameters derived from the motion tracking algorithms described in this study are those which are of importance for the quantitative evaluation of changes in the patients' movement during rehabilitation and are segment rotation (orientation tracking) and joint or segment trajectory (position tracking).

### B. Orientation Tracking

One key parameter in the assessment of limb function is the active range of motion (AROM). AROM usually refers to the voluntary range of movement around a specific joint. AROM provides information about the patients' ability to move and joint mobility [33]. The change in orientation of the upper limb segments with respect to their original displacement can be represented by the inertial sensors' Euler angle outputs (roll, pitch and yaw) in the global reference frame (Fig. 2 (a)). To perform the AROM test, the subjects were asked to move

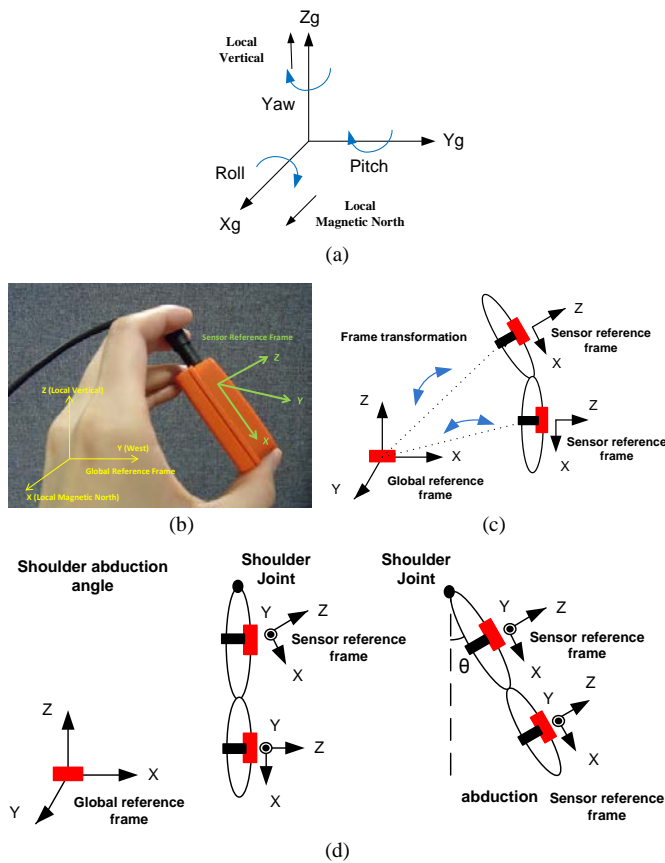


Fig. 2. The reference frame transformation (a) Euler angle in the global reference frame (b) Sensor and global reference frames (c) Frame transformation between sensor reference frame and global reference frame (d) Shoulder abduction in the global reference frame

their upper limb without any external assistance. The subjects were asked to perform 7 DoF rotation, including shoulder flexion-extension, internal-external rotation, adduction-abduction, elbow flexion-extension, forearm supination-pronation, wrist flexion-extension and ulnar-radius deviation. As seen in Fig. 2 (d), the pitch angle of the sensor attached on the upper arm is  $-90$  degrees to the initial displacement where the abduction angle is  $0$  degree. The direction of the abduction rotation is the same as that of the pitch angle, which is the rotation around the  $y$ -axis. Therefore according to the above relationship, the shoulder pitch angle (Fig. 2 (d)) is related to the pitch angle of the sensor attached on the upper arm as presented in equation (1). In this case the output of the pitch angle is presented in the global reference frame. The choice of reference frame will depend on how the data is to be presented - see section II.C.1.

$$\text{abduction angle} = \text{pitch angle} + 90^\circ \quad (1)$$

### C. Position Tracking

In order to explore the feasibility of using inertial sensors for segment position tracking, kinematic modelling and DR methods have been used. The flow chart for these tracking strategies is presented in Fig. 3. The kinematic model derives

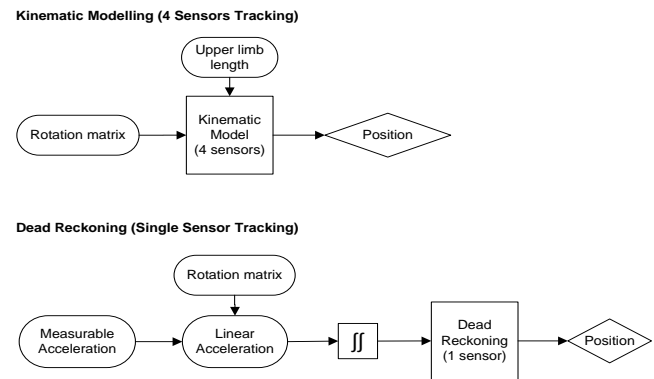


Fig. 3. Kinematic and Dead Reckoning position tracking strategies

the position of each upper limb segment from knowledge of the segment lengths and the orientation of the sensors on each limb segment. Multiple sensors are required to build up the kinematic model. DR uses double integration of the linear acceleration, the acceleration with the gravity component removed, to calculate changes in position of that sensor.

#### 1) Four Inertial Sensor Based Kinematic Model

Based on the upper limb kinematic geometry, the displacement of the multi-linked skeleton model of the upper limb can be described by the rotation of the upper limb segments about a reference point. For simplification, these segments have been treated as rigid bodies of fixed length whose deformation can be neglected. These segments, linked by joints, are treated as a kinematic chain.

To describe the relative positions of the segments, a common reference frame is necessary for each segment or sensor [34]. This reference system is usually defined with respect to the global reference frame or with respect to the sensor itself (sensor reference frame). In accordance with the right-handed co-ordinate system, the global reference frame is an earth-fixed reference frame (Fig. 2 (b)) whose positive  $X$  direction points to the local magnetic North, positive  $Y$  direction points to the West, and positive  $Z$  direction points in the opposite direction to the force of gravity. The sensor reference frame is fixed to the device in the right-handed co-ordinate system: the  $X$ -axis points horizontally to the right of the sensor, the  $Y$ -axis points upwards (vertical to the  $X$ -axis in the horizontal plane of the sensor) and the  $Z$ -axis points towards the outside of the sensor's horizontal plane as shown in Fig. 2 (b). To describe the movement trajectory of the upper limb segments, a common reference frame is required to present the relative movements of each upper limb segment. In order to be able to relate the outputs from all the sensors to the common reference frame, the measurements in the sensor reference frames have firstly to be converted into the global reference frame. This is achieved by the application of the Rotation Matrix [34] to the orientation output of the sensors. Fig. 2 (c) shows the frame transformation between the above two reference frames.

Though the global reference frame is well defined, it is conceptually easier to relate any segment motion to a reference point on the patient, especially as the patient may move relative to the global reference frame during or between measure-

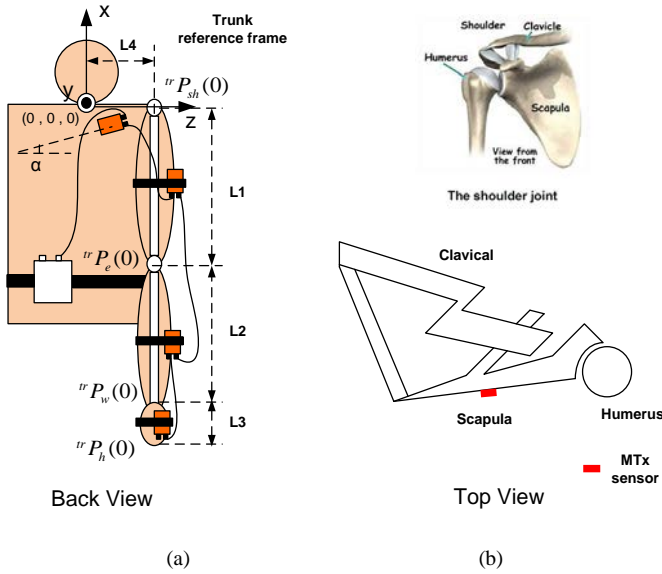


Fig. 4. Four-sensor kinematic model (a) 4 Sensor Model (b) Sensor's placement on shoulder [37]

ment sessions. Therefore in this preliminary evaluation the lowest vertebra of the neck is used as the reference point, as shown in Fig. 4 (a). The positive X-axis of the sensor is upward parallel to the axial skeleton of the upper limb, the positive Y-axis of the sensor points into the plane and the positive Z-axis points rightward corresponding to the right hand rule.

The kinematic model is based on that used for robotic manipulators [34] and a 7 Degree of Freedom (DoF) upper limb model [35] is used. The orientation data inputs to the kinematic model can be obtained directly from the MTx sensors, with each sensor being capable of producing orientation information in three formats (Euler angle, Rotation Matrix, and Quaternions [36]). In this study, the Rotation Matrix is used. Although movement of the shoulder is tracked by the sensor attached to the scapula it should be noted that the shoulder joint is very complex, consisting of three bones, the clavicle, scapula and humerus, with each possessing associated articulations [37]. The four-sensor model shown in Fig. 4 (a) assumes that the movement of the shoulder is caused solely by scapular movement (as shown in Fig. 4 (b)) with the trunk remaining stationary during movement.

The initial position of the shoulder  ${}^{tr}P_{sh}(0)$  relative to the reference point as shown in Fig. 4 (a), the elbow initial position  ${}^{tr}P_e(0)$  relative to the shoulder, the wrist initial position  ${}^{tr}P_w(0)$  relative to the elbow and the hand initial position  ${}^{tr}P_h(0)$  relative to the wrist in the trunk reference frame are expressed as  ${}^{tr}P_{sh}(0) = (-\cos \alpha * L4, \sin \alpha * L4, 0)^T$ ,  ${}^{tr}P_e(0) = (-L1, 0, 0)^T$ ,  ${}^{tr}P_w(0) = (-L2, 0, 0)^T$  and  ${}^{tr}P_h(0) = (-L3, 0, 0)^T$  in the trunk reference frame. Here, the lengths of the upper arm ( $L1$ ), forearm ( $L2$ ) and hand ( $L3$ ) are measured, thus defining the initial position of the elbow, wrist and hand as the constraints of the upper limb kinematic model with  $L4$  defined as the distance between the shoulder

and the reference point  $(0,0,0)$ . In order to estimate shoulder movement, the sensor was attached onto the scapula. The  $\alpha$  is the angle of this sensor with respect to the Z-axis in the trunk reference frame and is measured with a goniometer. In order to measure the length of the upper limb segments ( $L1$ ,  $L2$ ,  $L3$  and  $L4$ ), the subject sits upright with arms hanging down. A non-stretchable tape measure was used. The upper arm (humerus) length ( $L1$ ) was measured between the shoulder joint and the elbow. The forearm length ( $L2$ ) was measured between the elbow joint and the wrist joint. And the hand length ( $L3$ ) was measured between the wrist and the center of the palm. The angle  $\alpha$  and length ( $L4$ ) were measured after the sensor had been attached onto the shoulder.

In equation (2) below,  ${}^gR_e(t)$  is the rotation matrix which rotates the elbow joint vector from the sensor reference frame to the global reference. This is obtained from the sensor's rotation matrix output which is generated by the Xsens inertial sensor using the integrated data fusion algorithm XKF as discussed in Section II.  ${}^{tr}R_e(t)$  is the rotation matrix which rotates the elbow joint vector from the global reference frame to the trunk reference frame. The product of the above two matrices,  ${}^{tr}R_sR_e(t)$ , is defined as the rotation matrix which rotates the elbow vector from the sensor reference frame to the trunk reference frame. Similarly the rotation matrices which rotate the shoulder, wrist and hand vectors from the sensor reference frame to the trunk reference frame are  ${}^{tr}R_sR_{sh}(t)$ ,  ${}^{tr}R_sR_w(t)$ ,  ${}^{tr}R_sR_w(t)$  and  ${}^{tr}R_sR_h(t)$  respectively. In equation (3), the position outputs of the shoulder, elbow, wrist and hand in the trunk reference frame are  ${}^{tr}P_{sh}(t)$ ,  ${}^{tr}P_e(t)$ ,  ${}^{tr}P_w(t)$  and  ${}^{tr}P_h(t)$  respectively. The shoulder position, for example, is calculated by multiplying the shoulder rotation matrix  ${}^{tr}R_sR_{sh}(t)$  and the initial shoulder position in the trunk reference  ${}^{tr}P_{sh}(0)$ . Similarly, the position of the elbow  ${}^{tr}P_e(t)$ , wrist  ${}^{tr}P_w(t)$  and hand  ${}^{tr}P_h(t)$  are calculated according to equation (3).

$$\begin{cases} {}^{tr}R_{sh}(t) = {}^{tr}R_{sh}(t) * {}^gR_{sh}(t) \\ {}^{tr}R_e(t) = {}^{tr}R_e(t) * {}^gR_e(t) \\ {}^{tr}R_w(t) = {}^{tr}R_w(t) * {}^gR_w(t) \\ {}^{tr}R_h(t) = {}^{tr}R_h(t) * {}^gR_h(t) \end{cases} \quad (2)$$

$$\begin{bmatrix} {}^{tr}P_{sh}(t) \\ {}^{tr}P_e(t) \\ {}^{tr}P_w(t) \\ {}^{tr}P_h(t) \end{bmatrix} = \begin{bmatrix} \left\{ {}^{tr}R_{sh}(t) \right\} * \left\{ {}^{tr}P_{sh}(0) \right\} \\ \left\{ {}^{tr}R_e(t) \right\} * \left\{ {}^{tr}P_e(0) \right\} + \left\{ {}^{tr}P_{sh}(t) \right\} \\ \left\{ {}^{tr}R_w(t) \right\} * \left\{ {}^{tr}P_w(0) \right\} + \left\{ {}^{tr}P_e(t) \right\} \\ \left\{ {}^{tr}R_h(t) \right\} * \left\{ {}^{tr}P_h(0) \right\} + \left\{ {}^{tr}P_w(t) \right\} \end{bmatrix} \quad (3)$$

## 2) Single Inertial Sensor Based Dead Reckoning Method

In order to explore the feasibility of using a single sensor to track the movement of one upper limb segment e.g. the hand, the DR method is used.

a) *DR Method*

This method estimates the current position by adding the estimated change in position obtained from the double integration of the measured linear acceleration, with respect to time, to the previous estimate of the position. By using the rotation matrix  ${}^sR(t)$ , the measurable acceleration vector in the sensor reference frame  ${}^s\vec{a}(t)$  can be converted from the sensor reference frame to the global reference frame or to a reference frame of choice e.g. the trunk reference frame. Once the gravitational component of the acceleration,  $\vec{g}$ , has been removed then double integration of the linear acceleration data in the global reference frame  ${}^s\vec{a}_{linear}(t)$  should, in theory, enable any change in sensor or segment position to be estimated. The equations used to calculate the linear position are as follows:

$${}^s\vec{a}_{linear}(t) = {}^sR(t) * {}^s\vec{a}(t) - \vec{g} \quad (4)$$

$${}^s\vec{v}_{linear}(t) = \int_t {}^s\vec{a}_{linear}(t) dt \quad (5)$$

$${}^s\vec{p}_{linear}(t) = \int_t {}^s\vec{v}_{linear}(t) dt = \iint_t {}^s\vec{a}_{linear}(t) dt \quad (6)$$

Where,  ${}^s\vec{a}_{linear}$ ,  ${}^s\vec{v}_{linear}$  and  ${}^s\vec{p}_{linear}$  are the linear acceleration, velocity and position, respectively, in the global reference frame. These vectors can then be transformed into the trunk reference frame by multiplication with the trunk reference rotation matrix.

Although this tracking method seems straightforward, errors in the estimate of offsets in the acceleration, changes in these offsets over the measurement period and the presence of white noise in the acceleration data can lead to significant errors in the calculation of the velocity and displacement of the upper limb segment. Furthermore, errors in the sensor orientation calculations (here the rotation matrix is used) may introduce further errors into position estimation. It is therefore challenging to estimate translational movement based on acceleration measurements alone. Initial evaluation [38] and evidence from the literature [20] indicate that position estimation using DR is only expected to be acceptable for measurements over one or two seconds. Typical errors over ten or more seconds can be the order of meters. One reason for this limitation is that drift resulting from the integration of the error in the estimate of the acceleration offset is very difficult to remove. To minimize errors, optimization methods such as Kalman filtering [39], high pass filter, wavelet analysis and the Zero Velocity Update (ZUPT) method [22] are typically employed. A detailed description and evaluation of these drift correction methods for position estimation is beyond the scope of this paper. Therefore, in this paper, only the ZUPT method is evaluated as the selected assessment tests contain the required zero velocity intervals.

b) *Drift Correction Method*

The ZUPT is a standard drift correction method used in inertial navigation systems [40]. This method is based on the assumption that there are time intervals when the segment velocity is known to be zero. When the segment velocity is known to be zero, the offset error in the computed segment velocity can be measured and the segment velocity reset to zero. If it can be assumed that the drift in velocity (caused by integration of the error in the estimate of the offset in the acceleration) between the zero velocity intervals is linear then a correction for that drift between those intervals can also be made, thus further reducing the error introduced by the offsets and their changes with time. In order to detect the occurrence of zero velocity the double threshold method [41] is used. In this method the short time signal energy and zero crossing rates are used to estimate these two thresholds. Since the gyro is very sensitive to changes in orientation, it is considered to be the best sensor to indicate zero velocity using the equation  $s = gyro_y$ . The signal  $s$  is divided into time frames, each containing four samples. For each of the frames, the short time energy  $E_i$  ( $i$  is the discrete time) is calculated by equation (7):

$$E_i = \sum_{n=1}^N s_i^2(n) \quad (7)$$

Where,  $s_i = gyro_{yi}$

And the zero crossing rates (ZCR)  $Z_i$  are calculated by:

$$Z_i = \sum_{n=1}^N |\text{sgn}[s_i(n)] - \text{sgn}[s_i(n-1)]| \quad (8)$$

Where,  $\text{sgn}[s_i(n)] = \begin{cases} 1, & s_i(n) \geq 0 \\ 0, & s_i(n) < 0 \end{cases}$ .

After computing the short time energy, two thresholds, T1 and T2, in short time energy are set. These are used as upper and lower thresholds to detect the start-point and end-point of a movement epoch. Here movement epoch is defined as the movement between two zero intervals. The lower threshold T2 should be selected to be small enough to include every possible spike due to movement and the upper threshold should be chosen to exclude every possible spike due to noise. These two values are determined based on trial and error and are chosen to make sure the right maxima of the motion can be detected while at the same time eliminating the effect of the presence of noise in the signal. Another threshold, T3, is used on the zero crossing rates data to detect the zero points. An example of application of this drift correction method will be presented in the results. Additionally, this method can also be used to identify the start and end point of each individual element of the upper limb segment movement for the DR and the Kinematic models. This will enable the automatic timing measurement of these movements which will be of value when analysing patient performance.

#### D. Subjects

The tests were conducted in a quiet room, permitting the subject to feel relaxed and undisturbed. During the test, the subjects were asked to sit in front of a table as shown in Fig. 5. This study included 10 healthy volunteers (age 20 to 38, 8 men and 2 women) and a 41 year old female patient who had been diagnosed with fourth ventricular lesion extending to the cervical spine: associated hydrocephalus and brain stem compression that resulted in an upper limb disability. This patient was tested upon admission to the Neuro-Rehabilitation Unit and throughout her rehabilitation over a period of six months. During the tests, the patient remained in a wheelchair because of her underlying condition.

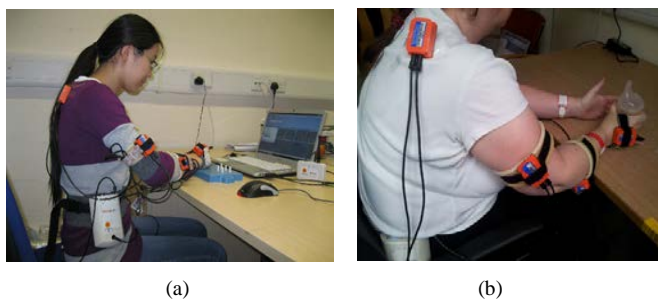


Fig. 5. Attachment of sensors to a subject (healthy volunteer or patient) (a) Sensors attached to a healthy volunteer (b) Sensors attached to a patient

#### E. Experimental Protocol

Experiments were carried out to validate the measurement system on volunteers and patients. The patient was tested once a week over a ten week period, and the assessment tests include the NHPT, Bean bag test, drinking water test, and AROM test. Each of the assessment tests was repeated three times. The NHPT is a standard rehabilitation assessment test commonly used to evaluate the dexterity of hand movement and grip (Fig. 6) [24]. The subject is asked to pick up the pegs from the bowl and place them into the holes. The time taken to complete the test is recorded using a stopwatch. Usually there is no requirement to insert the pegs in a fixed sequence, however, for initial evaluation of the system and to simplify the evaluation of the accuracy of the inertial measurement system - the distance between the holes is known - the subject was asked to insert the pegs into the holes in order from 1 to 9 (Fig. 6).

Although this requires hand and finger dexterity it also requires control of the shoulder, upper and lower arm. Additionally as the distance between each peg hole is known this was selected as one of the tests for evaluating the sensor systems. Therefore the aim of the experiments was to track upper limb segment rotation and position during known movements. Velfoam and Velcro were used to attach the MTx inertial sensors onto the subject's shoulder, upper arm, and forearm and hand respectively (Fig. 5). Velfoam was used to help minimize the discomfort of sensor attachment onto the upper limb and to stabilize the sensors attachment so that any movement relative to the limb segment is minimized. The lengths of the upper arm and forearm were measured as described in Section II.C.1

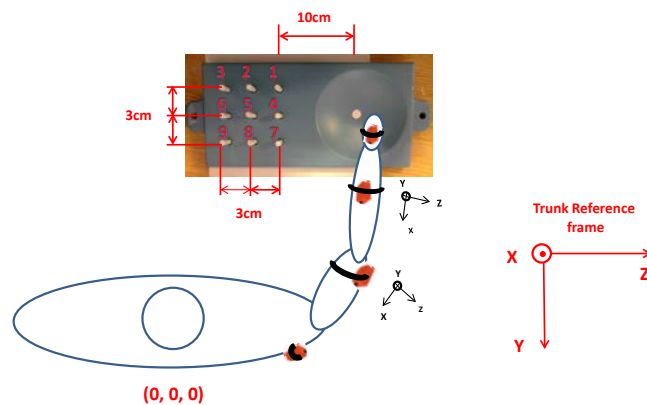


Fig. 6. Example of the NHPT

and used in the kinematic model and the uncertainty in the measurement of segment length is estimated to be 0.5 cm. The effect of error in the measurement of segment length and alignment of the sensors has also been evaluated. For example, a measurement error in upper arm length of 0.5 cm will cause an average position measurement error of 0.4 cm on x-axis, 0.1 cm on y-axis (the error on z-axis is smaller and therefore can be ignored) in a NHPT. Additionally, it should be noted that any relative movement between the clothes and the upper limb will also introduce errors in the position measurement. In practice it is estimated that during the tests the movement between the sensors and upper limb segments is less than 0.5 cm relative to its initial placement and at present is ignored. The sensors must also be aligned parallel with the skeleton axis of the upper limb segments within  $1^\circ$ . This presents no difficulty with healthy volunteers' who can straighten their arm, however, some patients are not able to straighten their arms. This makes it more difficult to align the sensors. Failure to align the sensors at the start of the measurement session will introduce uncertainty into the measurement of the relative joint and segment orientation and position. The expected alignment orientation presented using Euler angle should be  $(0, -90, \text{yaw}(\psi))$ . It is estimated that a  $1^\circ$  deviation in pitch and yaw will cause an error of 0.5 cm, 0.01cm, and 0.01cm with respect to all the three axes (x-axis, y-axis and z-axis) in the trunk reference frame with a 30 cm arm segment.

#### F. Accuracy Evaluation Protocol

Two assessment tests - the Active Range of Motion (AROM) test and the Nine Hole Peg Test (NHPT) - will be used in the system evaluation. Two parameters were selected as quantifiable measures of performance during the AROM test: (i) the measurement of AROM, and (ii) the time taken to perform the test. Both measurements provide the clinician with quantitative information about the progress of the patient throughout the rehabilitation programme.

##### 1) Orientation Tracking Accuracy Evaluation against a Goniometer

A goniometer was used to check the static orientation accuracy. Two MTx sensors were attached to the goniometer and the orientation then changed from 0 to 80 degree in 10 degree increments. The measurements were repeated for all four MTx

inertial sensors.

## 2) Position Tracking Accuracy Evaluation against a Vicon Camera System and a Goniometer

In order to evaluate the accuracy of the Xsens inertial position tracking system using kinematic modelling comparison was made using a Vicon motion capture system - whose accuracy is stated to be 0.1 mm. Preliminary tests were carried out on normal volunteers performing the Nine Hole Peg Test (NHPT). The elbow and wrist positions were tracked using a two sensor kinematic model to estimate elbow and wrist position. The experimental set-up is shown in Fig. 7 (a).

A second validation test used a goniometer to represent a simple two segment model of the upper limb. As presented in Fig. 7 (b), the right end of the goniometer represents the shoulder - which is fixed and in this case does not rotate - and the centre of the goniometer represents a 2D elbow joint and the left end of goniometer represents the wrist. In this basic 2D position tracking test, the right arm of the goniometer was fixed during the movement and the left section of goniometer rotated clockwise  $90^\circ$  in the vertical plane.

Because the accuracy of the sensors' alignment on the upper limb segments will affect the accuracy of tracking the upper limb joints position, calibration of the kinematic model before each measurement session is needed. It should be noted that the calibration procedures are the same for both the kinematic modelling and DR method. The calibration process takes 1 minute and requires the subject to be stationary with their arm hanging down in order to obtain the sensor rotation matrix in the sensor reference frame,  $R_{sensor}$ . The ideal sensor attachment is shown in Fig. 5 and the ideal orientation using the Euler angle is  $(0, -90, 0)$ . The value of yaw will depend on the patient's orientation with regard to the local magnetic north.

The corrected alignment rotation matrix  $R_{alignment}$  is calculated by the multiplication of expected orientation matrix,

$$R_{expected\ alignment} = \begin{bmatrix} 0 & 0 & -1 \\ 0 & 1 & 0 \\ 1 & 0 & 0 \end{bmatrix} \text{ and the sensors' alignment}$$

rotation matrix,  $R_{sensor}$  using equation (9).

$$R_{alignment} = R_{sensor} \otimes R_{expected\ alignment} \quad (9)$$

The corrected alignment rotation matrix,  $R_{alignment}$ , and the rotation matrix are used in the kinematic model to convert the measurements from sensor reference frame to the trunk reference frame.

## III. RESULTS

### A. Orientation and Position Tracking Accuracy

#### 1) Orientation Tracking Accuracy Evaluation against a goniometer

The experimental results in section II.F.1 show that the val-

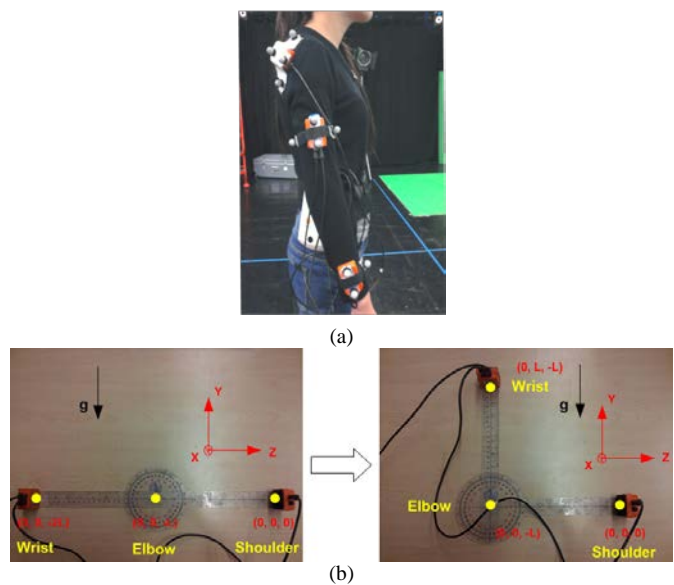


Fig. 7. System evaluation set-up (a) Vicon system set-up (b) Goniometer experimental set-up

ue of averaged roll, pitch and yaw for a rotation of  $80^\circ$  were within  $0.23^\circ$ ,  $0.23^\circ$  and  $0.46^\circ$ , indicating that the MTx measurement accuracy is within the manufacturer's specification of  $0.5^\circ$  for roll/pitch measurement is  $0.5^\circ$  and  $1.0^\circ$  for yaw [27].

#### 2) Position Tracking Accuracy Evaluation against a Vicon Camera System and a Goniometer

The experiment results in the section II.F.2 show that the mean error in position tracking was approximately 2 mm and the correlation of position tracking results between the Vicon system and the inertial sensing Xsens system is 99%. It can be seen from Fig. 8 (a), pgs 2, 4, 5, 6, 7, 8 and 9, that the position tracking result from both sensing systems visually correlate within 5 mm, which is an indication that the inertial system using the Xsens sensors and applying the kinematic model is working well enough for upper limb measurements. Also it should be noted that the peg pick up position for both Vicon and Inertial systems begins at around 9 cm and shows a variation of about 1 cm throughout the test. This could be due to shoulder movement, hand flexion about the wrist and differing positions of the pegs in the bowl. This uncertainty arises because only two sensor outputs were analysed for the inertial system and any shoulder, hand or finger movement could not be taken into account. But overall the movements of the upper and lower arm segments estimated by the two systems are the same within a few mm.

The change in position of the left end of the goniometer in the y-axis has been calculated using the kinematic model for the MTx in the initial sensor reference frame as shown in Fig. 8 (b). The expected movement of the end of the goniometer arm is 0 to 10 cm on the y-axis. The error in the measurement of a 10 cm movement was within 0.1 cm.

#### B. Active Range of Motion (AROM) Test

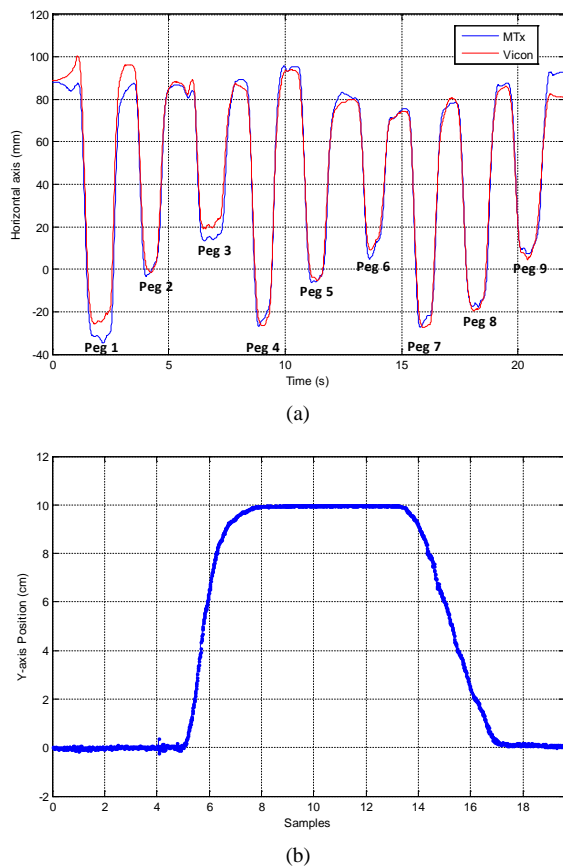


Fig. 8. Accuracy evaluation results (a) NHPT wrist position tracking by Vicon & Xsens (b) Position tracking result by Xsens

The AROM test was repeated three times at each session. In this paper, the measurement of the shoulder adduction range of motion has been selected as a typical example of the type of analysis that the inertial system can provide. In this test a single sensor is attached to the upper limb, and the subject then moves that limb away from the neutral position at the side of body. The normal range of shoulder abduction is expected to lie between  $160^\circ$  and  $180^\circ$  [42] though some claim that normative values for shoulder abduction are in the range from  $150^\circ$  to  $180^\circ$  [43] [44]. The healthy volunteers' values were found to range between  $140^\circ$  and  $170^\circ$ . The value of  $140^\circ$  lies outside the normative range and indicated the presence of dysfunction due to an initially undisclosed shoulder injury. The box-plot [45] of Fig. 9 (a) presents the weekly outcome of these tests for the patient over a ten week period. The patient repeated the assessment three times. The bottom and the top of the box are the minimum and maximum of the data. The red line in the plot represents the mean value.

It can be seen that at the beginning of the treatment, the patient's shoulder abduction range was  $60^\circ$ , which was significantly lower than that for the normative value. Over the treatment period it can be seen that, apart from weeks 5 and 6, the recovery follows an S shaped curve. During weeks 5 and 6 deterioration in performance is measured. The patient stated that she felt tired, unwell and also depressed. These events can explain the seeming deterioration in the patient's range of mo-

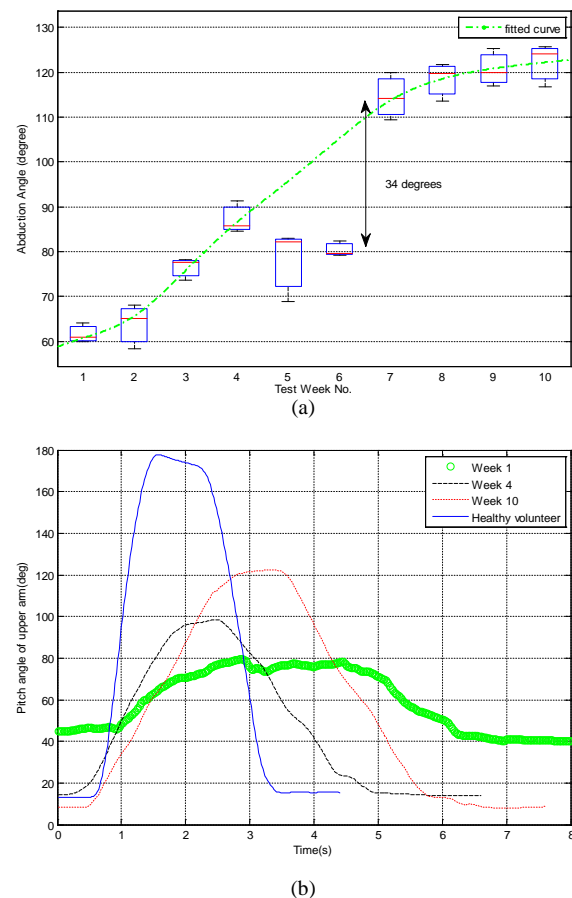


Fig. 9. Shoulder abduction test on healthy volunteer and patient (a) Patient's shoulder abduction plotted against test week number (b) Shoulder abduction range of motion plots of patient and healthy volunteer

tion. However it can be seen that at week 7 the range of motion returns to the recovery curve and that the previous period has not impacted on overall recovery. Furthermore, it can be seen that after week 8 the range of movement begins to stabilize at around  $120^\circ$ . This reduction in rate of improvement may indicate that the patient had reached the limit of expected range of shoulder abduction and that treatment could now be stopped or that an alternative treatment regime is required. The attainment of a  $120^\circ$  degree range of motion is significant for the patient as this indicates that some basic functional activities are now practical (e.g. to comb one's hair requires a shoulder abduction angle of  $112^\circ \pm 10^\circ$ ).

An example of time series data is shown in Fig. 9 (b) where the pitch angle of the upper arm is plotted against time for the patient in weeks 1, 4 and 10 of treatment and also for a typical healthy volunteer. This data indicates that not only is there an increase in the range of motion during the rehabilitation program, but also a decrease in the time taken for the patient to complete the task. Although there is an improvement in the patient's performance, it can be seen that the test still takes the patient twice as long to complete compared to a healthy volunteer. Additionally there is evidence from the reduced smoothness of the curves that the patient has a lower level of fine motor control compared with healthy volunteers. This loss of

fine motor control has been reported in a previous study on movement smoothness in stroke patients [46].

Although a goniometer can be used to measure the final value for range of movement, it limits the patient to a two dimensional measure of motion and cannot provide information on the dynamic change in orientation or a more detailed timing analysis. Whereas the inertial sensor system can provide three dimensional dynamic information on how the motion is achieved as well as a more detailed timing analysis. This additional information may be of clinical value.

**C. The Nine-Hole Peg Test**

**1) Position Estimation Using Kinematic Modelling Based Multiple Inertial Sensors System:**

Four sensors are attached onto the arm segments as shown in Fig. 6. Fig. 10 shows the hand and shoulder position estimation using kinematic modelling in the x, y and z axes in the trunk reference frame. In Fig. 10 the hand position on the z-axis represents horizontal hand movement. In this axis the peg positions for holes 1, 4, and 7 should have the same value. The position tracking result of Fig. 10 (a) indicates that this is the case. In Fig. 10 (a) the pegs 1, 4, 7; pegs 2, 5, 8 and pegs 3, 6, 9 have similar magnitudes (within 0.6 cm) on the z-axis while the pegs 1, 2, 3; pegs 4, 5, 6 and pegs 7, 8, 9 have similar magnitudes (within 0.7 cm) on the y-axis. The x-axis result represents the vertical movement of the measurement seg-

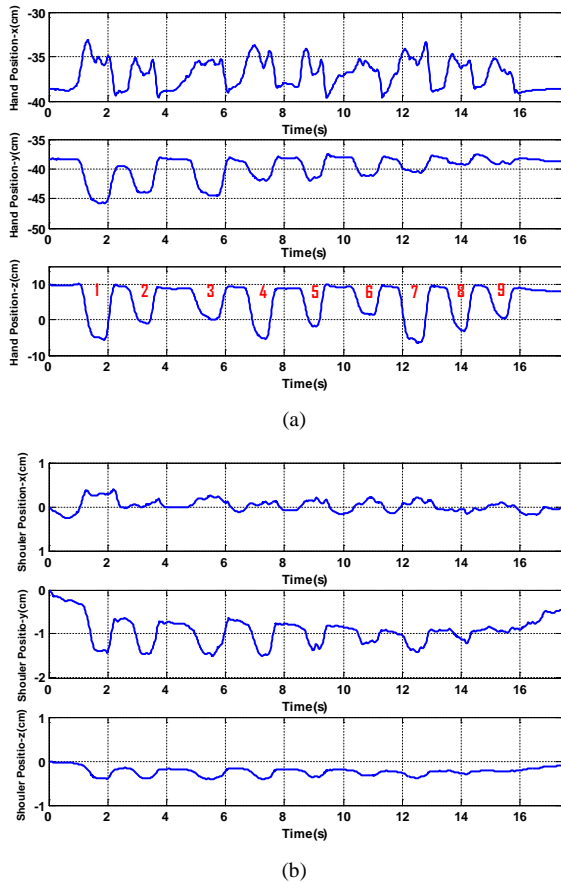


Fig. 10. Hand and shoulder position tracking on 3-axis of NHPT (a) 3D hand position tracking of NHPT (b) 3D shoulder position tracking of NHPT

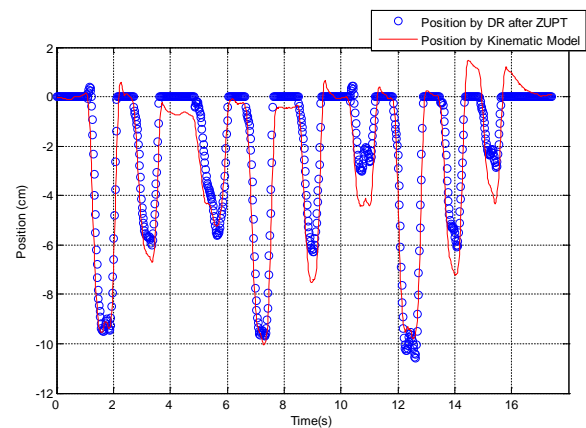
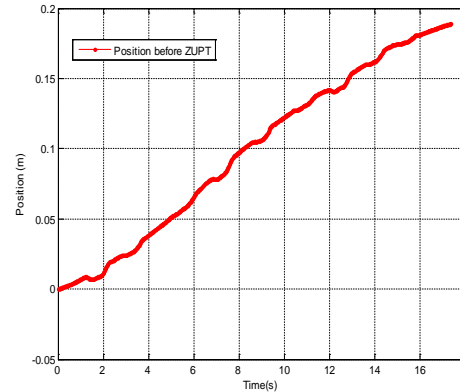
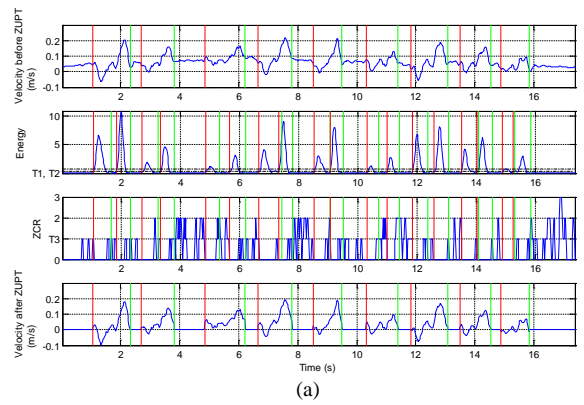


Fig. 11. Comparison of wrist position tracking by using dead reckoning (with or without ZUPT drift correction method) and kinematic modelling for the nine-hole peg test (a) ZUPT algorithm with velocity before and after it (b) Position tracking plot before ZUPT (c) Position tracking comparison between DR and kinematic model

ment. It can also be seen that the wrist position does not have the same value every time it returns to the origin to pick up the next peg.

**2) Position Estimation by Using the DR Method and a Single Inertial Sensor:**

For the NHPT test, using the DR method, the initial position for a healthy volunteer's hand movement in the horizontal direction in the trunk reference frame is plotted in Fig. 11 (b). As can be seen, if offsets in the acceleration are not corrected

then the drift in the estimation of position is very large, reaching a magnitude approximately 20 times larger than the original value within 20 seconds of beginning the test. However, as the hand velocity will be zero at peg pick up and peg insertion and the ZUPT correction method discussed in section II.C.2.b can be applied.

The red line and green line shown in Fig. 11 (a) represent the start and end of each peg insertion movement. As described in Section II.C.2.b, using the threshold values T1, T2 (two thresholds of short time energy) and T3 (threshold of zero crossing rates), the spikes in gyro energy data are detected as shown in the middle graph in Fig. 11 (a). Since one of the features is that the spikes in velocity signal correspond to the spikes in the gyro energy, the start and end points in velocity signal can be figured out. This algorithm starts from the first frame (according the short term energy), the comparison initially will be made between the low threshold value T2 and the short time energy. If the first point N1 exceeds the threshold value T2 but the next point after N1 does not exceed value T2, this point cannot be treated as start point. If point N1 exceeds the high threshold value T1, N1 is the first start point. The same method is applied for detecting the end point N2 as well. The red line indicates the start point while the green line indicates the end point. The first and last plot in Fig. 11 (a) presents the velocity data before and after the ZUPT.

Fig. 11 (b) shows the uncorrected position tracking result. Fig. 11 (c) shows the comparison between the DR and kinematic models. Applying the ZUPT algorithm to the DR method has reduced the error to 0.8%, an acceptable level.

However this basic application of the ZUPT algorithm does introduce an error as movement data is discarded within the detected zero intervals and so the DR data will underestimate the actual movement.

### 3) Position Tracking Comparison between the Healthy Volunteer and Patient

A series of measurements were carried out using the four sensor kinematic model system. Fig. 12 (a) shows typical position tracking on the horizontal axis (Z-axis in the trunk reference frame) for a nine-hole peg test for a healthy volunteer in contrast to a typical result from the patient in Fig. 12 (b). It is evident that there is significant base line movement (5 - 10 cm) during the peg placement for the patient. This is thought to be caused by compensatory movement of the shoulder by the patient in order to achieve the task. It can also be seen that the time taken to place each peg can be measured. This data can be analysed to identify differences between the timing patterns of a normal subject and the patient [47].

These results provide evidence that the use of the inertial measurement system provides the clinician with data which is not only objective but also can provide further insight into the dynamic movements and their characteristics throughout the assessments.

## IV. DISCUSSION & CONCLUSION

In this paper, the preliminary evaluation of two systems utilising inertial sensors has been presented. One system utilises a four-sensor and a kinematic model, the second a single sen-

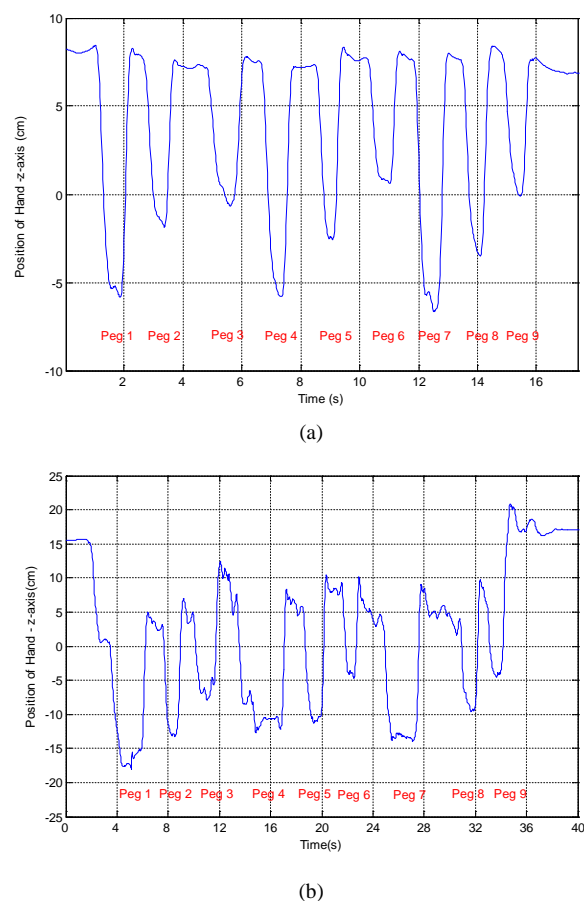


Fig. 12. Healthy volunteer and patient's horizontal position data of nine-hole peg test (a) Healthy volunteer's horizontal position tracking result (b) Patient's horizontal position tracking result

sor and the Dead Reckoning method. This second system has been evaluated as it is hoped that the use of a single sensor for more basic Range of Motion measurements and where measurement of the movement of a single segment is acceptable.

The system using Kinematic modelling has been compared with the Vicon system and shown to provide accurate position tracking within 0.1 cm over a distance of 10 cm, but at least two sensors are required to construct the kinematic model. If only the movement of a single segment is required, then in terms of system cost and set-up in a clinical setting, a single sensor system using the DR method with ZUPT correction is an option. Initial evaluation of correction techniques, such as the ZUPT, has indicated that it may be possible to reduce the effect of these errors to an acceptable level (0.8% of the total movement distance). However this rather crude use of the ZUPT has removed some of the movement data as it corrects the errors and further refinement is needed. It should also be noted that the use of ZUPT requires the zero intervals in the assessment tests. Additionally for some tests e.g. the NHPT, the distance between the peg locations is known and this data can also be used to help reduce any modelling errors.

In this research, a preliminary evaluation has been carried out on 10 healthy volunteers and one patient. The performance of this patient was tracked over 6 months from the day admitted to the hospital to the day discharged. Additional infor-

mation such as dynamic information and compensatory movements has been provided by these two systems in different assessment tests. In the AROM test, the inertial systems are able to provide dynamic position and orientation data against time. The monitoring of all the segments also allows the clinician to know whether a patient is successfully completing a test through using compensatory movements. For example, in the patient's NHPT, the variation in base line movement was too great to be explained by finger movement and is probably due to the patient using trunk - which is assumed to be the stable reference frame - and shoulder movement to compensate for limited arm mobility. However this pattern indicates that if the reference frame is not stable, its movement can be deduced - as can the source of the compensatory movement. This could be important in understanding how the patient is recovering function, even if the test is completed within the expected normal time range. In addition the plots indicate that the healthy volunteer finds it easier than the patient to return to the center of the peg container to pick up the next peg. This also implies that the volunteer has better control of the upper limb segments than the patient. As it can be seen from the Fig. 12, the healthy volunteer's movement is smoother, there is minimal trunk movement and the test takes less time to finish.

Therefore this information should provide the clinician with additional information on clinical recovery and this may also motivate the patient to his/her rehab prescription. Larger translational trials are now required to assess the validity and usability of these inertial measurement systems.

#### REFERENCES

- [1] "Neuro Numbers: a brief review of the numbers of people in the UK with a neurological condition," *The Neurological Alliance*, 2003.
- [2] C. Goldsmith, *Neurological disorders*, Blackbirch Press, 2001.
- [3] G. Kwakkel, B. J. Kollen, J. van der Grond and A. J. Prevo, "Probability of Regaining Dexterity in the Flaccid Upper Limb : Impact of Severity of Paresis and Time Since Onset in Acute Stroke," *Stroke*, vol. 34, pp. 2181-2186, 2003.
- [4] T. Platz, C. Pinkowski, F. V. Wijck, I. H. Kim, P. D. Bella and G. Johnson, "Reliability and validity of arm function assessment with standardized guidelines for the Fugl-Meyer Test, Action Research Arm Test and Box and Block Test: a multicentre study," *Clin. Rehabil.*, vol. 19, pp. 404-411, 2005.
- [5] "Box and Block Test," [Online]. Available: <http://www.rehastim.de/cms/index.php?id=122>.
- [6] R. C. Lyle, "A performance test for assessment of upper limb function in physical rehabilitation treatment and research," *Int J Rehabil Res.*, vol. 4, pp. 483-492, 1981.
- [7] D. J. Gladstone, C. J. Danells and S. E. Black, "The Fugl-Meyer Assessment of Motor Recovery after Stroke: A Critical Review of Its Measurement Properties," *Neurorehabil Neural Repair.*, vol. 16, pp. 232-240, 2002.
- [8] J. H. Van der Lee, H. Beckerman, G. J. Lankhorst and L. M. Bouter, "The Responsiveness of the Action Research Arm Test and the Fugl-Meyer Assessment Scale in Chronic Stroke Patients," *J Rehabil Med.*, vol. 33, pp. 110-113, 2001.
- [9] N. F. Gordon, M. Gulanick, F. Costa, G. Fletcher, B. A. Franklin, E. J. Roth and T. Shephard, "Physical activity and exercise recommendations for stroke survivors," *Circulation*, vol. 109, pp. 2031-2041, 2004.
- [10] J. W. Krakauer, "Motor learning: its relevance to stroke recovery and neurorehabilitation," *Curr Opin Neurol.*, vol. 19, pp. 84-90, 2006.
- [11] T. B. Moeslund, A. Hilton and V. Kruger, "A survey of advances in vision-based human motion capture and analysis," *Computer Vision and Image Understanding*, vol. 104, pp. 90-126, 2006.
- [12] D. Roetenberg, C. T. Baten and P. H. Veltink, "Estimating Body Segment Orientation by Applying Inertial and Magnetic Sensing near Ferromagnetic Materials," *IEEE Trans. Neural Syst. Rehabil. Eng.*, vol. 15, pp. 469-471, 2007.
- [13] H. M. Schepers, "Ambulatory Assessment of Human Body Kinematics and Kinetics," the Netherlands, 2009.
- [14] B. Kaushik and D. Nance, "A Review of the Role of Acoustic Sensors in the Modern Battlefield," in *11th AIAA/CEAS Aerocoustics Conference*, 2005.
- [15] K. Maenaka, "MEMS inertial sensors and their applications," in *Proceeding of the 5th International Conference on Networked Sensing Systems*, Kanazawa, Japan, June 17-19, 2008.
- [16] H. Zhou, T. Stone, H. Hu and N. Harris, "Use of multiple wearable inertial sensors in upper limb motion tracking," *Med Eng Phys.*, vol. 30, pp. 123-133, 2008.
- [17] B. Hingtgen, J. McGuire, M. Wang and G. Harris, "An upper extremity kinematic model for evaluation of hemiparetic stroke," *J Biomech.*, vol. 39, pp. 681-688, 2006.
- [18] J. C. Perry, J. Rosen and S. Burns, "Upper Limb Powered Exoskeleton Design," *IEEE-ASME Trans. on Mechatronics*, vol. 12, pp. 408-417, 2007.
- [19] L. Ojeda and J. Borenstein, "Non-GPS navigation for emergency responders," in *Proceedings of International Joint Topical Meeting: Sharing Solutions Emergencies Hazardous Environment*, Salt Lake City, February, 2006.
- [20] D. Titterton and J. Weston, "Strapdown Inertial Navigation Technology (2nd Edition)," the American Institute of Aeronautics and Astronautics, 2004.
- [21] E. Foxlin, "Pedestrian Tracking with Shoe-Mounted Inertial Sensors," *IEEE Comput. Graph. Appl.*, vol. 25, no. 6, pp. 38-46, 2005.
- [22] L. Ojeda and J. Borenstein, "Personal Dead-reckoning System for GPS-denied Environments," in *IEEE International Workshop on Safety, Security, and Rescue Robotics (SSRR2007)*, Rome, Italy, September 27-29, 2007.
- [23] I. Skog, P. Handel, J.-O. Nilsson and J. Rantakokko, "Zero-Velocity Detection-An Algorithm Evaluation," *IEEE Trans. Biomed. Eng.*, vol. 57, pp. 2657-2666, 2010.
- [24] V. Mathiowetz, K. Weber, N. Kashman and G. Volland, "Adult norms for the Nine Hole Peg Test of finger dexterity," *Occup Ther J Res.*, vol. 5, pp. 24-38, 1985.
- [25] B. Smoot, J. Wong, B. Cooper, L. Wanek, K. Topp, N. Byl and M. Dodd, "Upper extremity impairments in women with or without lymphedema following breast cancer treatment," *J Cancer Surviv.*, vol. 4, pp. 167-178, 2010.
- [26] G. Hansson, I. Balogh, L. Rylander and S. Skerfving, "Goniometer measurement and computer analysis of wrist angles and movements applied to occupational repetitive work," *J Electromyogr Kinesiol.*, vol. 6, pp. 23-35, 1996.
- [27] "Xsens Company," [Online]. Available: <http://www.xsens.com>.
- [28] S. L. Wolf, A. J. Butler, L. Alberts and M. W. Kim, "Contemporary linkages between EMG, kinetics and stroke rehabilitation," *J Electromyogr Kinesiol.*, vol. 15, pp. 229-239, 2005.
- [29] A. D. Pandyan, P. Vuadens, F. M. van Wijck, S. Stark, G. R. Johnson and M. P. Barnes, "Are we underestimating the clinical efficacy of botulinum toxin (type A)? Quantifying changes in spasticity, strength and upper limb function after injections of Botox® to the elbow flexors in a unilateral stroke population," *Clin. Rehabil.*, vol. 16, p. 654-660, 2002.
- [30] G. Alon, A. F. Levitt and P. A. McCarthy, "Functional Electrical Stimulation Enhancement of Upper Extremity Functional Recovery During Stroke Rehabilitation: A Pilot Study," *Neurorehabil Neural Repair.*, vol. 21, pp. 207-215, 2007.
- [31] H. Zhou and H. Hu, "Human motion tracking for rehabilitation-A survey," *Biomed. Signal Process. Control*, vol. 3, pp. 1-18, 2008.
- [32] MT Manager User Manual, Document MT0216P, Revision F, Xsens Technologies B.V., 27 May 2009.
- [33] H. Clarkson, "Musculoskeletal assessment: joint range of motion and manual muscle strength (2nd Edition)", Philadelphia: *Lippincott Williams & Wilkins*, 2000.
- [34] J. Craig, "Introduction to robotics: mechanics and control," 1989.

- [35] J. Yang, K. Abdel-Malek and K. Nebel, "Reach Envelope of a 9-Degree-of-Freedom Model of the Upper Extremity," *Int J Robot Autom.*, vol. 20, pp. 240-259, 2005.
- [36] S. O. H. Madgwick, "An efficient orientation filter for inertial and inertial/magnetic sensor arrays," 2010.
- [37] V. M. Zatsiorsky, "Kinematics of human motion, *Human Kinetics*," 1998.
- [38] L. Bai, M. G. Pepper, Y. Yan, S. K. Spurgeon, M. Sakel and M. Phillips, "A Multi-parameter assessment tool for upper limb motion in neurorehabilitation," In *Proc. IEEE International Instrumentation and Measurement Technology Conference (I2MTC 2011)*, pp. 21-24. 2011.
- [39] H. Luinge and P. Veltink, "Measuring orientation of human body segments using miniature gyroscopes and accelerometers," *Med. Biol. Eng. Comp.*, vol. 43, p. 273-282, 2005.
- [40] J. Huddle, "Trends in inertial systems technology for high accuracy AUV navigation, AUV'98," in *Proc. of the 1998 Workshop on Autonomous Underwater Vehicles*, 1998.
- [41] J. Vartiainen, J. J. Lehtomaki and H. Saarnisaari, "Double-threshold based narrowband signal extraction," in *Proc. of the IEEE Vehicular Technology Conference (VTC)*, 2005.
- [42] "Shoulder Abduction," 26 09 2012. [Online]. Available: [http://www.lhup.edu/yingram/jennifer/webpage/shoulder\\_goniometry.htm](http://www.lhup.edu/yingram/jennifer/webpage/shoulder_goniometry.htm).
- [43] "Range of Joint Motion Evaluation Chart," [Online]. Available: [http://www.dshs.wa.gov/pdf/ms/forms/13\\_585a.pdf](http://www.dshs.wa.gov/pdf/ms/forms/13_585a.pdf).
- [44] "Shoulder abduction normative value," 26 09 2012. [Online]. Available: [http://www.endurancecorner.com/Alan\\_Couzens/functional\\_flexible\\_swim](http://www.endurancecorner.com/Alan_Couzens/functional_flexible_swim).
- [45] D. F. Williamson, R. A. Parker and J. S. Kendrick, "The box plot: a simple visual method to interpret data.," *Annals of Internal Medicine*, vol. 110, no. 11, pp. 916-921, 1989.
- [46] B. Rohrer, S. Fasoli, H. I. Krebs, R. Hughes, B. Volpe, W. R. Frontera, J. Stein and N. Hogan, "Movement Smoothness Changes during Stroke Recovery," *J. Neurosci.*, vol. 22, no. 18, p. 8297-8304, 2002.
- [47] A. K. Mithal, "Using Psychomotor Models of Movement in the Analysis and Design of Computer Pointing Devices," in *Proc. of the CHI*, 1995.



**Lu Bai** received the B.Eng. degree in Biomedical Engineering from Tianjin University, Tianjin, P.R. China in 2009 and the Ph.D. degree in Electronic Engineering from University of Kent, U.K in 2014.

Her primary research interest is 3D human upper limb motion tracking for rehabilitation purpose. She is now a visiting Post-doctoral researcher of School of Engineering and Digital Arts at University of Kent.



**Matthew G. Pepper** received the B.Sc. and Ph.D. degrees in Applied Physics from University of Kent, Canterbury. He is Senior Lecturer in Medical Instrumentation at the University of Kent, Kent, U.K., and Consultant Clinical Scientist in the Medical Physics Department, Kent and Canterbury Hospital. His main research interests are in the area of Rehabilitation Engineering, focussing on Electronic Assistive Technology for independent mobility and communication. Current projects include the development of driving

assistance systems for powered wheelchairs and vision based devices for accessing assistive technology.



**Yong Yan** (M'04-SM'04-F'11) received the B.Eng. and M.Sc. degrees in instrumentation and control engineering from Tsinghua University, Beijing, China in 1985 and 1988, respectively, and the Ph.D. degree in flow measurement and instrumentation from the University of Teesside, Middlesbrough, U.K., in 1992.

He was an Assistant Lecturer with Tsinghua University in 1988. In 1989, he joined the University of Teesside as a Research Assistant, where he was a Lecturer from 1993 to 1996, after a short period of

postdoctoral research. He was a Senior Lecturer, Reader, and Professor with the University of Greenwich, Chatham Maritime, U.K., from 1996 to 2004. He is currently a Professor of Electronic Instrumentation, the Head of Instrumentation, Control and Embedded Systems Research Group, and the Director of Research the School of Engineering and Digital Arts, the University of Kent, Canterbury, U.K. He has published in excess of 300 research papers in journals and conference proceedings.



**Sarah K. Spurgeon** received the B.Sc. and D.Phil. degrees from the University of York, York, U.K., in 1985 and 1988, respectively.

She has held academic positions at the University of Loughborough and the University of Leicester in the UK and is currently Professor of Control Engineering and Head of the School of Engineering and Digital Arts at the University of Kent. She is a member of the Editorial Board of the International Journal of Systems Science, a member of the Editorial Board of the IET Proceedings D, a Subject Editor for the International Journal of Robust and Nonlinear Control and an Editor of the IMA Journal of Mathematical Control and Information. Her research interests are in the area of robust nonlinear control and estimation, particularly via sliding mode techniques in which area she has published in excess of 300 refereed papers. Professor Spurgeon received the IEEE Millennium Medal in 2000 and was awarded the 2010 Honeywell International Medal in recognition of her outstanding contribution to control theory and systems engineering. She is a Fellow of the IET, a Fellow of the IMA, a Fellow of the InstMC, was elected a Fellow of the Royal Academy of Engineering in 2008.



**Mohamed Sakel** leads the East Kent NeuroRehabilitation Unit at Canterbury as its Director & Consultant Physician. He advises the government funding bodies for neuro-rehab service provision for a County. His clinical and research interest includes rehabilitation and Neuro-modulation of brain injury, stroke, spasticity, Brain Computer Interface, Minimally Conscious State. He provides the Botox service for adults in East Kent since 2003. He published and completed multiple research projects on spasticity, patient experience, MND. He has completed several multi-national researches with UK, US, Canada & EU countries. He was the audit lead for the Medical Directorate up to 2009. He regularly organises multidisciplinary conferences.

His current research grants include MRC funding for post-stroke spatial-neglect and 2 EU funded for "intelligent wheelchair" & Robotics. He holds honorary Senior Research Fellow position in Electronic Engineering & Senior Lecturer in Psychology at the University of Kent.

He was an elected member of the Medical Academic Staff Committee of BMA (UK) for 2012-14. He was the Director for R & D of the East Kent University hospital and an executive member of the Kent County regional Research network Board from 2008-2012.



**Malcolm Phillips** received the Ph.D. degree in Physiological Measurement from University of Kent in 2000. He has previously worked at the University of Kent and in Industry. He is Lead Clinical Engineer in Medical Physics, East Kent Hospitals Trust and visiting lecturer in the School of Engineering and Digital Arts at the University of Kent. He has responsibility for the safety and governance of all medical devices within the Trust and is the Trust's qualified person regarding the design and manufacture of Medical Devices, including those used for research purposes. He is a member of the Trust's Medical Devices Group and the Information Development Group, where he provides advice on governance, safety and future trends/strategy regarding medical devices.